Available online at www.sciencedirect.com
ScienceDirect
Diamond & Related Materials 17 (2008) 937–943
DIAMOND AND RELATED MATERIALS
www.elsevier.com/locate/diamond

TEM and Raman characterisation of diamond micro- and nanostructures in carbon spherules from upper soils

Z.Q. Yang [a,1], J. Verbeeck [a], D. Schryvers [a,*], N. Tarcea [b], J. Popp [b], W. Rösler [c]

[a] EMAT University of Antwerpen, Groenenborgerlaan 171, B-2020 Antwerp, Belgium
[b] Institut für Physikalische Chemie, Friedrich-Schiller-Universität Jena, Helmholtzweg 4, D-07743 Jena, Germany
[c] Institute for Pre- and Early History, University of Mainz, Schillerstrasse 11, D-55116 Mainz, Germany

Received 28 September 2007; received in revised form 14 January 2008; accepted 24 January 2008
Available online 13 February 2008

Abstract

Carbonaceous spherules of millimeter size diameter and found in the upper soils throughout Europe are investigated by TEM, including SAED, HRTEM and EELS, and Raman spectroscopy. The spherules consist primarily of carbon and have an open cell-like internal structure. Most of the carbon appears in an amorphous state, but different morphologies of nano- and microdiamond particles have also been discovered including flake shapes. The latter observation, together with the original findings of some of these spherules in crater-like structures in the landscape and including severely deformed rocks with some spherules being embedded in the fused crust of excavated rocks, points towards unique conditions of origin for these spherules and particles, possibly of exogenic origin.

Keywords: Diamond nanoparticles; Diamond microflakes; Carbon spherules; Impact

1. Introduction

On Earth, elemental carbon is produced as the result of a variety of biogenic or pyrogenic processes, usually leading to graphitic forms of carbon or to diamond when more extreme thermo-mechanical conditions exist. Extraterrestrial carbon may survive atmospheric entry [1,2] and the occurrence of high pressure/high temperature polymorphs, such as diamond or fullerene-like forms of carbon may be indicative for impact events [3,4,5]. Here we report on the finding of a new type of spherule-shaped, mm-sized, carbonaceous particle in soils, wide-spread over Europe, with particular microscopic features, content and physical properties. In total about 70 samples were collected of which 65 from forest top soils and 5 from grassland or swamp, mostly throughout Europe with the emphasis on SE Bavaria (Germany) (35 samples) and Austria. In the few cases when the samples did not contain any spherules, local mechanical disturbances over the years were identified that could have destroyed the delicate structures.

In the present paper results from samples collected near Burghausen (Germany) and Spa (Belgium) are presented, but similar results have been obtained from selected samples from other areas. However, it should be clear that particular observations are not necessarily representative for every individual spherule, i.e. in some spherules no crystalline material was observed. The focus of the present paper is on the micro-, nano and atomic structure of the crystalline structures found inside the spherules, the physical properties will be discussed in a forthcoming publication.

2. Experimental procedures

The mm-sized particles further-on called spherules, although they clearly do not have perfect spherical shapes as can be seen from Fig. 1, were collected from soil samples from areas with low mechanical disturbance of the top soil like forest soils or soils from swamp areas. The examples shown in Fig. 1 are typical for all spherule findings in the different locations.

* Correspoding author.
E-mail address: nick.schryvers@ua.ac.be (D. Schryvers).
[1] Now at College of Materials Science and Engineering, Hunan University, Changsha, Ch-410082, China.

0925-9635/$ - see front matter © 2008 Elsevier B.V. All rights reserved.
doi:10.1016/j.diamond.2008.01.104

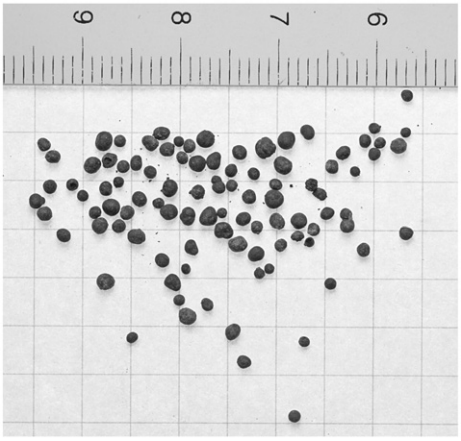

Fig. 1. Batch of millimeter sized black particles found near Burghausen (Germany). The shapes, sizes and distribution are typical for this and other locations.

The size of the spherules typically varies between 0.1 and 1.5mm. For the present microscopy measurements, different sample preparation techniques have been employed including crushing and polishing. In most cases and for ease of use, relatively large spherules have been selected and embedded in a resin for polishing with SiC paper. Hollow as well as completely filled spherules have been found, but in most cases a typical open cell- or foam-like structure as shown in the optical micrograph of Fig. 2 was observed. After mechanical polishing, some samples were further thinned by Ar^+ ion-milling for transmission electron microscopy (TEM) characterization. The latter was performed in a CM20 Philips instrument equipped with a thin window INCA x-sight energy dispersive X-ray (EDX) detector and in an UltraTwin CM30 Philips FEG instrument equipped with a post-column GIF2000 electron energy-loss spectroscopy (EELS) detector.

Due to the dark coloration and the fragile texture of the sample the Raman measurements were performed with extreme small laser powers at the sample position (approx 0.01mW). The spherules were broken into small pieces and the scans were performed on the exposed inner surfaces. A 632nm red laser was used with the light focused down to a spot of around 2μm diameter with an Olympus MPlan x50 objective. Scattered light was collected with the same objective and analyzed with a LabRam HR 800 spectrometer from Jobyn Yvon. The spectra were recorded with a Peltier cooled CCD camera. Raster scanning over large areas (100 × 100μm) of the sample was performed using an automatic microscopic stage.

3. Results

Scanning electron microscopy (SEM) confirms the foam- or cell-like internal structure of the cenospheres with cell sizes of a few micron. Elemental compositions obtained from EDX show a high portion of carbon but also considerable amounts of oxygen and only on a few occasions some iron and silicon is measured. In the ion-milled TEM samples the cell structures can still be recognized as seen from the low-magnification image of Fig. 3. At these and moderate magnifications the matrix of these structures seems to consist of amorphous material with possible variations in density or thickness, but when zooming in to higher magnifications small nanoparticles with diameters below 5nm are recognized as shown in Fig. 4a. From the high resolution TEM (HRTEM) image of a selected nanoparticle shown in Fig. 4b the typical lattice projection along a <110> direction of an fcc crystal, as can also be concluded from the accompanying diffractogram, can be recognized while in Fig. 4c a highly defected particle, or a coagulation of even smaller particles, is observed. Typical lattice spacings of 0.2 and 0.18nm can be measured from these HRTEM lattice images. In Fig. 5 the electron energy-loss near edge structure (ELNES) spectrum with a carbon K-edge of an area containing a large concentration of these nanoparticles is shown. This spectrum essentially shows a small π* pre-edge and a main σ* edge with some detail resembling the typical shape of the diamond ELNES although a genuine diamond pattern should reveal sharper peaks [6]. In the inset the low-loss energy loss spectrum is shown revealing a peak around 24eV.

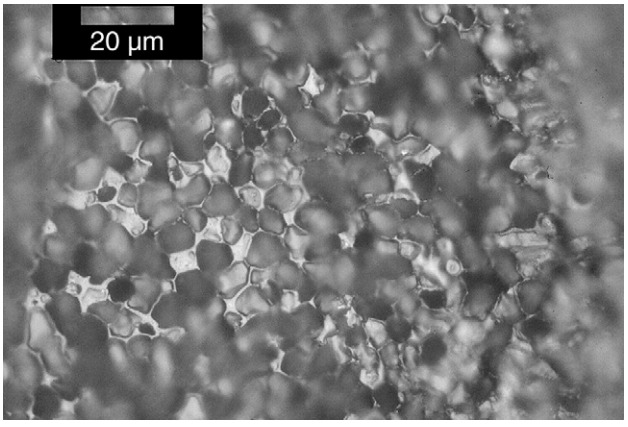

Fig. 2. Optical micrograph of a mechanically polished particle showing the typical micrometer sized cell-like structure inside the particles.

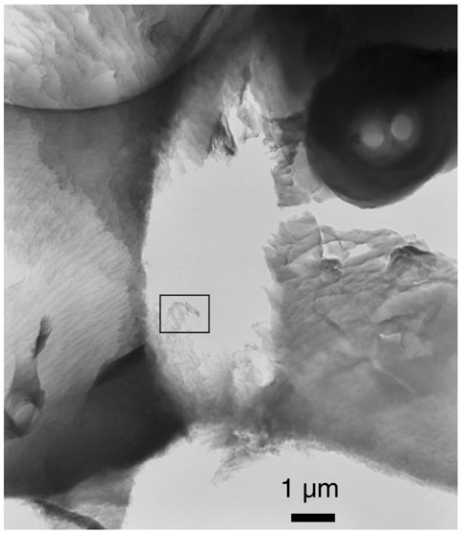

Fig. 3. Low-magnification TEM micrograph showing a seemingly amorphous structure with possible density fluctuations.

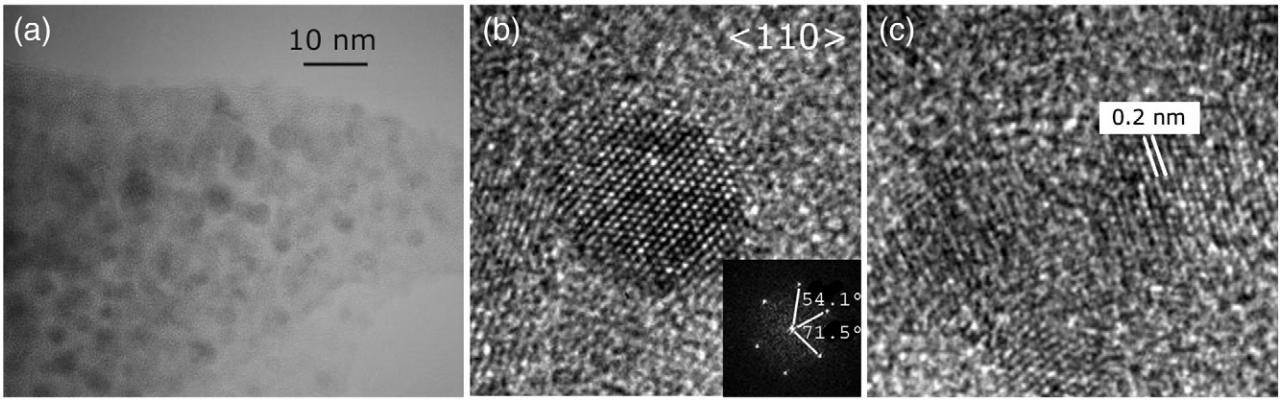

Fig. 4. (a) Overview of the indicated region in Fig. 3 revealing an area of nanoparticles. (b) HRTEM of a single fcc nanoparticle seen along the <110> direction and (c) of a highly defected particle still revealing the omnipresent lattice spacing of 0.2 nm.

In other areas or other samples contiguous areas of highly defected fcc based nanograins with sizes between 10 and 50nm are observed. In Fig. 6a a dark field (DF) image is shown together with the corresponding selected area electron diffraction (SAED) ring pattern including the used aperture and the indexing of the rings. In Fig. 6b a HRTEM image of such a contiguous area reveals multiple defects and local lattice deformations. The lattice parameters obtained from the rings in the SAED pattern of Fig. 6 are listed in Table 1 and correspond well with those of the nanoparticles in Fig. 4. EDX from these areas only reveals carbon and oxygen. Fig. 7 shows the ELNES of such a domain, which now only shows a typical amorphous carbon K-edge [6] with some small additional fringes superposed on the tail of the σ* edge possibly due to the crystalline material.

In a few specimens, micrometer-sized, flake-shaped crystalline particles could be identified within the cell-like structures as shown in Fig. 8. From the curved shapes of the particles in Fig. 8a the anisotropy of their morphology is clear, i.e. they extend over several hundreds of nanometers to even a micrometer in one or two directions while in the third direction they are extremely thin with an estimated thickness around 50nm. In Fig. 8b the normal to the main surface is shown by the SAED inset revealing a <111> zone and several nanoparticles are found embedded in an amorphous surface layer surrounding the microcrystal. Fig. 8c shows a HRTEM image along a [110] zone revealing a properly resolved lattice with in the inset a filtered part of the image revealing two opposite edge dislocations. Corresponding SAED patterns are presented in Fig. 9 revealing typical [001], [110] and [111] cubic patterns and an example of an ELNES spectrum of the carbon K-edge for such a microparticle is given in Fig. 10, including a low-loss spectrum with a peak around 33eV. From the diffraction patterns again the same lattice parameters as above can be measured.

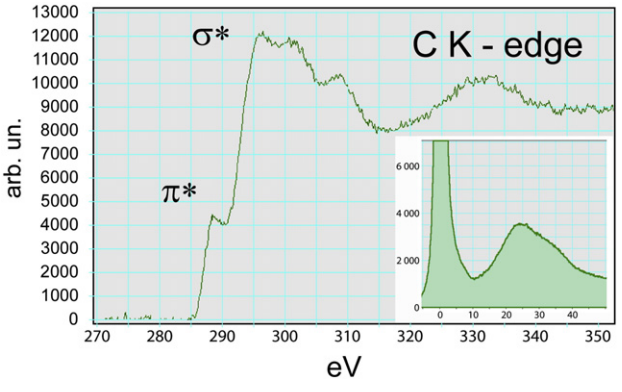

Fig. 5. ELNES of the carbon K-edge of an area containing nanoparticles embedded in their original amorphous support. The inset shows the low-loss region with a peak around 24 eV.

In Fig. 11a the Raman spectrum of a typical spherule is shown, revealing two bands at 1290cm^{-1} and 1590cm^{-1} known as the D and G band complexes, respectively. These and other observed spectra are characteristic for amorphous carbon and distorted graphitic structures [7]. The band in the middle (1467cm^{-1}) could possibly be attributed to carbon atoms in spherical surroundings as in C_{60} molecules or nanotubes [8]. The Raman spectrum shown in Fig. 11b reveals a sharp peak at 1332.3cm^{-1} with a FWHM of ~ 6cm^{-1} which can be attributed to a relatively large diamond particle with a minimal volume of approximately (100nm)^3 inside the spherule [9,10].

4. Discussion

From the analytical data it is clear that the crystalline nanoparticles, nanograins as well as microparticles primarily consist of carbon, the larger the particles the smaller the oxygen content in the spectrum. The latter indicates that the oxygen primarily originates from the amorphous surroundings, which can be the embedding matrix for the nanoparticles or a surface layer for the nanograins and microparticles, although some amorphous fillings in the nanograin structure of Fig. 6 can be expected. In all observed cases, the overall cubic symmetry of the lattice and the measured lattice parameters correspond well to those of diamond [see, e.g., 11] but also to those of fcc carbon which has a reported lattice parameter of 0.3563nm [12,13,14]. In view of the present precision, no lattice expansion for the nanoparticles with respect to bulk material could be measured. For a perfect cubic diamond crystal the 200 reflections or diffraction ring should be extinct, which is not always the case in the present electron diffraction data. Still, 200 reflections are known to

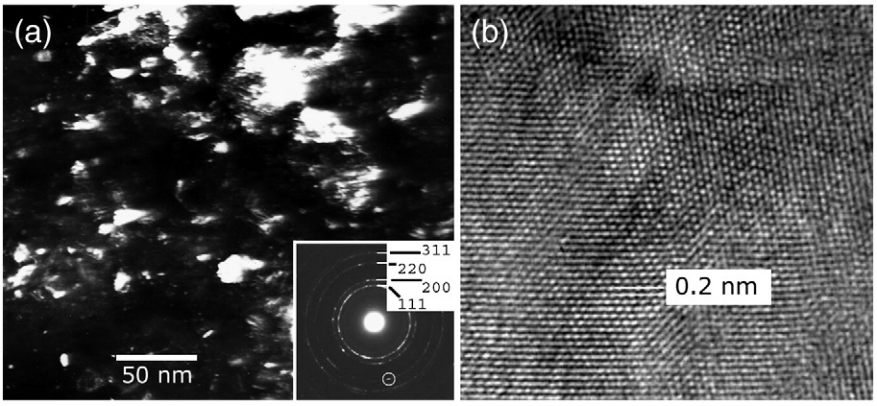

Fig. 6. (a) Dark field of a contiguous area of nanograins together with the corresponding SAED ring pattern including the used aperture. (b) HRTEM image of an area as seen in (a) and revealing several lattice defects and distorted zones.

appear in diamond electron diffraction patterns due to multiple diffraction or possible numerous small deviations from the perfect cubic symmetry thus violating the extinction conditions for a perfect diamond lattice or by streaks appearing from the existence of multiple planar defects [15]. Certainly the lattice defects clearly exist in the case of the nanoparticles and -grains, as seen from, e.g., figs. 4c & 6b, respectively. Moreover, the [001] zone pattern of the microparticles shown in Fig. 9a indeed misses the 200 reflections as indicated by crosses, proving the extinction character of these positions and thus the cubic diamond nature of the microflakes.

As for the energy loss spectra, the shape of the σ* edge in the ELNES pattern of the microparticle as seen in Fig. 10 is characteristic for the sp^3 bonding of 4 coordinated atoms in the three-dimensional network of tetrahedrons in diamond. Indeed, comparing the spectrum of Fig. 10 with typical reference ELNES spectra for different types of carbon [see e.g. 6,12,16,17] the characteristic triple peaks within 15eV of the onset followed by a large hump around 330eV stands out. Also the low-loss peak at 33eV confirms the diamond structure (app. C in ref. [6]). The small π* edge which can be seen in front of the σ* edge in the experimental pattern of Fig. 10 but not in the calculated ones of diamond [see, e.g., 18] can be attributed to an amorphous carbon layer or the presence of C=C chains at the surface of nano- or microdiamonds or attributed to surface damage [17,19,20,21]. Moreover, the Raman spectrum shown in Fig. 11b revealing the sharp peak at 1332.3cm^{-1} confirms the existence of relatively large diamond particles [9].

In other words, for the larger microparticles it is clear that these have the regular cubic diamond structure. Moreover, so far no twinning or other lattice defects have been observed in these flake-shaped particles. However, the smaller the particles become, the less clear the distinction between diamond and fcc carbon can be made. The 200 extinction in diamond can be violated due to many lattice defects, the characteristic ELNES blurred by the amorphous embedding matrix and the <110> HRTEM for thin samples under certain imaging conditions not resolving the dumbbells in a Si-type structure is very similar to that of fcc carbon. Still, the shape of the ELNES of Fig. 5 is sufficiently distinguishable from the one of fcc carbon to rule out that possibility for the nanoparticle morphology: indeed, the three peaks followed by the broader hump in the σ* edge in the ELNES of the nanoparticles in Fig. 5 clearly point towards diamond. The shift of the low-loss peak to the lower energies around 24eV can be explained by the decrease in size accompanied by the increase in surface plasmon content and depends on the actual size but also on the shape of the particles (ch. 3.3.5 in [6]). Incidentally, this plasmon energy is very close to that of fcc carbon, which was measured and calculated at 22eV [22,23], but the shape of the core-loss of fcc carbon does not show the characteristic sp^3 detail (Fig. 3 in [12]) so the latter remains the most important feature to identify the nanoparticles as also having the diamond structure. The slightly fainter detail in the observed spectrum can be explained by a limited long range order and a possibly slightly strained structure of the nanoparticles, next to the embedding amorphous carbon.

Table 1
Measured interplanar spacings (±0.001 nm) from the SAED ring pattern in Fig. 6 compared to literature values for diamond [11]

Hkl	Measured *d* value (nm)	Literature *d* value (nm) for diamond
111	0.207	0.206
200	0.180	0.178
220	0.126	0.126
311	0.109	0.108

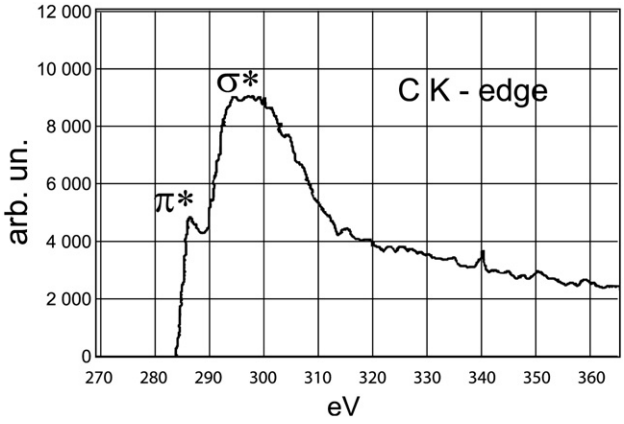

Fig. 7. ELNES of the carbon K-edge of a nanograin domain.

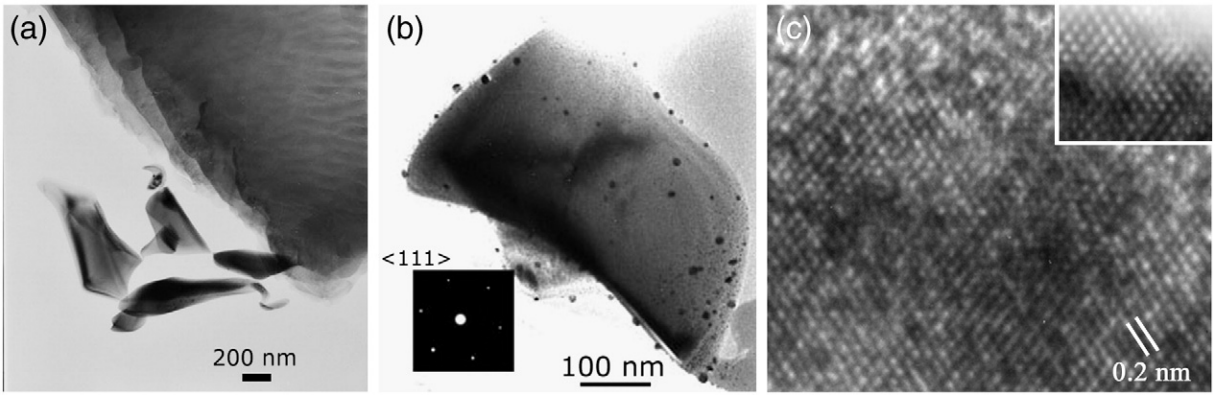

Fig. 8. Several examples of micrometer sized flake-shaped particles including the <111> zone for the normal to the surface of the flake in (b). (c) HRTEM image of the edge of a microflake observed along a [110] zone including inset showing an edge dislocation.

As for the nanograins, the situation is less clear. Although there is no obvious reason why one would expect a different crystallographic structure for this morphology, the ELNES, electron diffraction nor the HRTEM are conclusive on any of both cubic structures, diamond or fcc carbon. One could argue that the characteristic high intensity tail in the carbon K-edge core-loss spectrum for fcc carbon as observed by Konyashin et al. [12] is clearly not existing in the present spectra, as these are dominated by a lower tail from the amorphous carbon. However, on the other hand, one would expect some more typical diamond sp^3 detail in the case of regular diamond, even when containing large amounts of lattice defects. The conclusion for the nanograins thus remains somewhat ambiguous, although all experimental observations can still be explained within the assumption of the diamond structure, taking a severely defected structure into account.

Here it should be indicated that the crystalline particles or areas are not observed in all investigated spherules. However, TEM is not a particularly suited technique for statistical studies due to the destructive nature and lengthy procedures for sample preparation and the present work is only intended to indicate the existence of these particles in some spherules, not to obtain data on the distribution over the different collection sites.

To our knowledge, these type of spherules have not been described in the literature before and are not known from anthropogenic or biogenic sources. The present occurrence is independent from local geology and possibly points to a regional high or intermediate energy process which would be necessary for the formation of the observed diamond particles. Moreover, the first findings of the spherules was made in the context of small-scale crater-like structures in the landscape and including severely deformed rocks with some spherules being embedded in the fused crust of excavated rocks [24,25]. In this respect an impact related origin of the spherules with a local or cosmic carbon source cannot be ruled out.

Although the internal microstructure of the spherules may differ slightly (some have an open core while others are completely filled with cells and in some the cell structure is homogeneous while in others the outer rim is much denser than the internal part) the cell- or foam-like structure is a constant feature. Such a structure suggests a rapid and high temperature event in which the original material has melted and evaporated in a fragmented way so as to produce mesopores of a few microns in size yielding the cell structure upon cooling. If this entire process occurs during a blast, i.e. while the molten droplets are in open space or air, the outer shape of the final particle is indeed expected to be close to spherical due to the primarily isotropic conditions of the environment.

As for the micro- and nanocrystalline material found inside the spherules, the strong difference in size and appearance

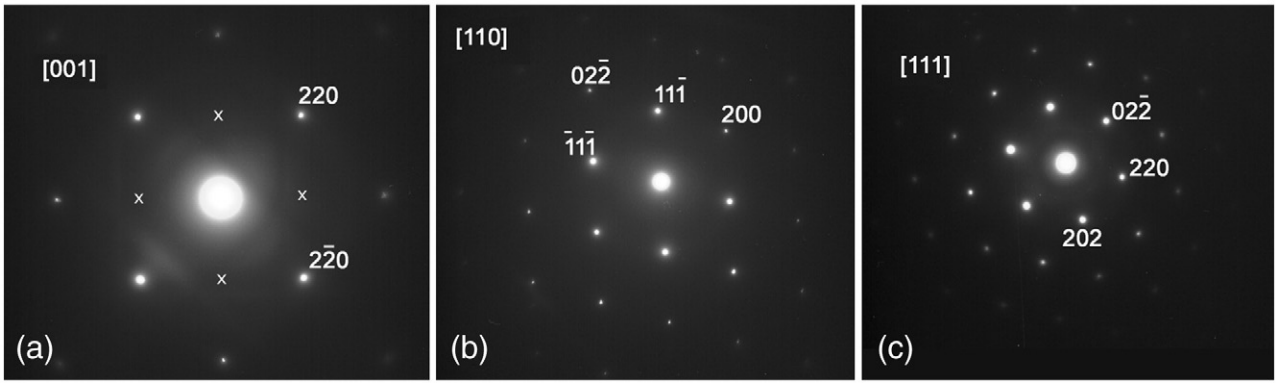

Fig. 9. Typical single crystal SAED patterns of different flake-shaped particles in different zones: (a) [001] zone with indications of diamond extinctions, (b) [110] zone and (c) [111] zone.

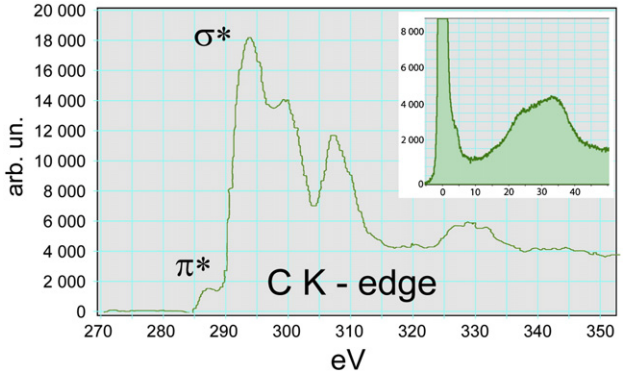

Fig. 10. ELNES of the carbon K-edge of a flake-shaped particle. The inset shows the low-loss region with a peak around 33 eV.

possibly points to a different origin and formation. First of all, according to Daulton et al. [26], diamond nanoparticles resulting from detonation typically reveal multiple planar twins as well as the polymorph of Lonsdaleite, both of which were not unambiguously observed in the present study. Also, such particles would result from a martensitic-like transformation of a graphite precursor of which also no remnants were found in the present study. In other words, the scenario of nanodiamond being formed by a solid-state transformation from graphite due to an explosion upon or before impact cannot be confirmed. More probably, the nanoparticles could have been formed by ablation of carbon material followed by a chemical vapor deposition (CVD) type of growth during and after the impact, in which case a lower fraction of twinning and Lonsdaleite would exist. In this case, also the nanodiamonds would have been created relatively recently, since the spherules are found in the upper layer of the Earth's soil dating this event between about one and two millennia back in time. However, the same process is also known to occur in interstellar space so the diamond nanoparticles can already have been existing in the impactor upon arrival, and thus being much older, and simply been distributed by the explosion. The latter case also corresponds with findings of meteorite nanodiamonds in acid-residues of the Allende and Murchison meteorites [26,27]. The fact that no multiply twinned nanoparticles have been observed might indicate that in the present case not many pentagonal or icosahedral symmetries existed in the CVD seed nuclei [26]. The possibility of the CVD process as being at the origin of the diamond particles could also be a possible reason for the still remaining question with respect to the nanograin material, as the androgenic fcc carbon material can also be produced by a CVD process [22].

Still, some of the defected nanoparticles or distorted nanograins might contain signatures as found in impact diamonds and the flake shape of the microparticles could be traced back to dense zones in a shock wave front yielding a <111> close packed plane normal in the direction of the propagation of the shock wave or it could be a remnant of a flat sheet of graphite [28]. A similar reasoning would be in place for the possibility of high velocity grain-grain collisions behind supernova shock waves, in which case the diamond particles would have been formed in interstellar space a long time before the impact on Earth [29,30]. To what extend such a natural process is capable of producing microflake crystals of diamond is unclear, although it is known from experiment that even at relatively low temperatures (i.e., in the range between 500°C and 700°C) such crystals can be formed by CVD, be it by starting from polymer precursors [31]. In the CVD concept, the <111> diamond epitaxy can be expected on the (0001) graphite plane, so the diamond microflakes could have been grown on existing graphite crystals or sheets [32]. The observed dislocations could be due to interfacial strain between the graphite substrate and the diamond film [26,33] Also, defect-free euhedral shaped diamonds up to 200nm in length have been observed at the Henbury impact site, Australia, for which also CVD formation was suggested [34].

However, although the first findings of the present carbon spherules were related to the above mentioned crater-like landscape structures and severely deformed rocks possibly pointing towards a high energy impact, the present microstructural observations cannot unambiguously prove an exogenic origin. Indeed, it is not impossible that, for example, a local volcanic eruption could produce or eject similar spherules containing diamond nano- and microstructures. The collection of similar particles over a large area in Europe would, however, imply an eruption event of a relatively large size. Similar conclusions and comments have recently been presented on seemingly analog structural findings, although the latter were dated around 12,900years ago as they were found in much deeper sediments [35]. It is clear that the present observations only reveal the first layer of raw data on these fascinating objects and that much more

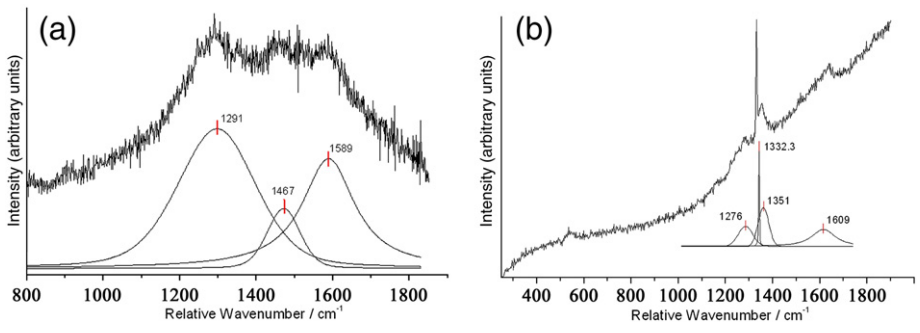

Fig. 11. (a) Typical Raman spectrum of a spherule interior showing amorphous carbon, distorted graphite and carbon atoms in spherical surroundings and (b) of a spherule showing a diamond peak at 1332.3 cm^{-1}.

work with many different characterization techniques needs to be done to elucidate the origin and formation of these spherules and their contents.

5. Conclusions

By using different transmission electron microscopy techniques (SAED, HRTEM, EELS) it was shown that the crystalline particles, nano- as well as micro-sized, observed inside mm-sized carbonaceous spherules found in upper soils throughout Europe, are diamond, although for some highly defected nano-grain areas the fcc carbon structure cannot be excluded. Raman spectroscopy confirms the existence of relatively large diamond particles. In view of the original findings of these spherules, it is suggested that they may have been formed during a high pressure/temperature event possibly related to an exogenic phenomenon not yet known. Based on the lack of clear twinning defect structures and the missing of any Lonsdaleite, it is suggested that the contained diamond nano- and microstructures have been formed by a chemical vapor deposition type process. Whether this would have occurred during or before any impact is still unclear for now.

Acknowledgements

Viktor Hoffmann from the University of Tübingen, Germany, and Bert Raeymaekers from Infraserv Gendorf, Burgkirchen, Germany, are gratefully acknowledged for their original input, stimulating discussions and continued interest in the matter. Z.Q. Yang is supported by a GOA project "Characterization of nanostructures by means of advanced EELS and EFTEM" from the University of Antwerp while J. Verbeeck is supported by the ESTEEM project. Dirk Lamoen and Mehrdad Dadsetani are acknowledged for support with the interpretation of the ELNES data.

References

[1] D.E. Brownlee, D.J. Joswiak, M.E. Kress, S. Taylor, J. Bradley, Lunar and Planetary Science Conference LPSC XXXIII (2002) Abs. #1786.
[2] M.E. Kress, D.E. Brownlee, R. Gammon, D. Joswiak, Meteoritics & Planetary Science 37 (2002) A82.
[3] B.M. French, Traces of Catastrophe LPI, Contribution No. 954., 1998, p. 102.
[4] V.L. Masaitis, Meteoritics & Planetary Science 33 (1998) 349.
[5] P.R. Buseck, Earth & Planetary Science Letters 203 (2002) 781.
[6] R.F. Egerton, Electron Energy-Loss Spectroscopy in the Electron Microscope, Plenum Press, New York, 1996.
[7] K. Nakamura, M. Fujitsuka, M. Kitajima, Physical Review. B 41 (1990) 12260.
[8] S. Lefrant, I. Baltog, M. Baibarac, J. Schreiber, O. Chauvet, Physical review. B 65 (2002) 235401.
[9] S.A. Solin, A.K. Ramdas, Physical Review. B 1 (1970) 1687.
[10] W. Rösler, V. Hoffmann, B. Raeymaekers, Z.Q. Yang, D. Schryvers, N. Tarcea, "Carbon spherules with diamonds in soils", 40th ESLAB Symposium; Abstracts of the first International Conference on Impact Cratering in the Solar System 08-12 May 2006, Noordwijk (NL).
[11] R.C. Weast (Ed.), Handbook of Chemistry & Physics, p. E-101, CRC Press, Cleveland Ohio, USA, 1975-1976, 56th edition.
[12] I. Konyashin, A. Zern, J. Mayer, F. Aldinger, V. Babaev, V. Khvostov, M. Guseva, Diamond and Related Materials 10 (2001) 99.
[13] S. Endo, N. Idani, R. Oshima, K.J. Takano, M. Wakatsuki, Physical Review. B 49 (1994) 22.
[14] S.M. Jarkov, Ya.N. Titarenko, G.N. Churilov, Carbon 36 (1998) 595.
[15] L. Nistor, V. Teodorescu, J. Van Landuyt, V. Ralchenko, in: Ludek Frank (Ed.), proc. EUREM 12 vol. II, Brno, Czech Republic, 2000, p. 495.
[16] J. Yuan, L.M. Brown, Micron 31 (2000) 515.
[17] J. Bruley, D.B. Williams, J.J. Cuomo, D.P. Pappas, Journal De Microscopie 180 (1995) 22.
[18] A.-L. Hamon, J. Verbeeck, D. Schryvers, J. Benedikt, Journal of Materials Chemistry 14 (2004) 2030.
[19] K. Okada, K. Kimoto, S. Komatsu, S. Matsumoto, Journal of Applied Physics 93 (2003) 3120.
[20] S. Evans, Reactivity of diamond surfaces, in: G. Davies (Ed.), Properties and growth of diamond, EMIS Datareviews Series, vol. 9, INSPEC, London, 1994, p. 64.
[21] D. Vanderbilt, S.G. Louie, Physical Review. B 30 (1984) 6118.
[22] I. Konyashin, V. Khvostov, V. Babaev, M. Guseva, J. Mayer, A. Sirenko, International Journal of Refractory Metals & Hard Materials 24 (2006) 17.
[23] M. Dadsetani, A. Pourghazi, Diamond & Related Materials 15 (2006) 1695.
[24] V. Hoffmann, W. Rösler, A. Patzelt, B. Raeymaekers, P. Van Espen, Meteoritics & Planetary Science 40 (2005) A69.
[25] W. Rösler, A. Patzelt, V. Hoffmann, B. Raeymaekers, "Characterisation of a small crater-like structure in SE Bavaria, Germany"; 40th ESLAB Symposium; Proceedings of the first International Conference on Impact Cratering in the Solar System 08-12 May 2006, Noordwijk (NL), pp 67–71.
[26] T.L. Daulton, D.D. Eisenhour, T.J. Bernatowicz, R.S. Lewis, P.R. Buseck, Geochimica et Cosmochimica Acta 60 (1996) 4853.
[27] R.S. Lewis, M. Tang, J.F. Wacker, E. Anders, E. Steel, Nature 326 (1987) 160.
[28] F. Langenhorst, Bulletin of Czech Geological Survey vol. 77 (2002) 265.
[29] D.F. Blake, F. Freund, K.F.M. Krishnan, C.J. Echer, R. Shipp, T.E. Bunch, A.G. Tielens, R.J. Lipari, C.J.D. Hetherington, S. Chang, Nature 332 (1988) 611.
[30] A.G.G.M. Tielens, C.G. Seab, D.J. Hollenbach, C. McKee, Astrophysical Journal Letters 319 (1987) L103.
[31] Z. Sun, X. Shi, B.K. Tay, X. Wang, Y. Sun, Thin Solid Films 308–309 (1997) 159.
[32] T. Suzuki, M. Yagi, K. Shibuki, M. Hasemi, Applied Physics Letters 65 (1994) 540.
[33] W. Luyten, G. Van Tendeloo, S. Amelinckx, J.L. Collins, Philosophical Magazine A 66 (1992) 899.
[34] Y. Ding, D.R. Veblen, American Mineralogist 89 (2004) 961.
[35] R. Firestone, A. West, J.P. Kennett, L. Becker, T.E. Bunch, et al., Proc. Nat. Acad. Sciences (PNAS) 104 (41) (October 2007) 16016.